ACS OMEGA

http://pubs.acs.org/journal/acsodf

Article

Plugging Characteristics and Evaluation Predicting Models by Controllable Self-Aggregation Nanoparticles in Pore Throat Microcapillaries

Zhiguo Yang, Xiangan Yue,* Minglu Shao, and Shanshan Gao

Cite This: *ACS Omega* 2023, 8, 21305−21314

Read Online

ACCESS | Metrics & More | Article Recommendations

ABSTRACT: Injecting nanoparticle profile agents into low-permeability heterogeneous reservoirs to plugging water breakthrough channels is a widely used technical method to enhance oil recovery. However, insufficient research on the plugging characteristics and prediction models of nanoparticle profile agents in the pore throat has led to a poor profile control effect, short profile control action time, and poor injection performance in the actual reservoir. This study uses controllable self-aggregation nanoparticles with a diameter of 500 nm and different concentrations as profile control agents. Microcapillaries of different diameter sizes were used to simulate the pore throat structure and flow space of oil reservoirs. Based on a large number of cross-physical simulation experimental data, the plugging characteristics of controllable self-aggregation nanoparticles in the pore throat were analyzed. Gray correlation analysis (GRA) and gene expression programming algorithm (GEP) analysis were used to determine the key factors affecting the resistance coefficient and plugging rate of profile control agents. With the help of GeneXproTools, the evolutionary algebra 3000 was selected to obtain the calculation formula and prediction model of the resistance coefficient and plugging rate of the injected nanoparticles in the pore throat. The experimental results show that the controllable self-aggregation nanoparticles will achieve effective plugging when the pressure gradient is greater than 100 MPa/m in the pore throat, and when the injection pressure gradient is 20−100 MPa/m, the nanoparticle solution will be in the aggregation to breakthrough state in the pore throat. The main factors affecting the injectability of nanoparticles, from strong to weak, are as follows: injection speed > pore length > concentration > pore diameter. The main factors affecting the plugging rate of nanoparticles, from strong to weak, are as follows: pore length > injection speed > concentration > pore diameter. The prediction model can effectively predict the injection performance and plugging performance of controllable self-aggregating nanoparticles in the pore throat. The prediction accuracy of the injection resistance coefficient is 0.91, and the accuracy of the plugging rate is 0.93 in the prediction model.

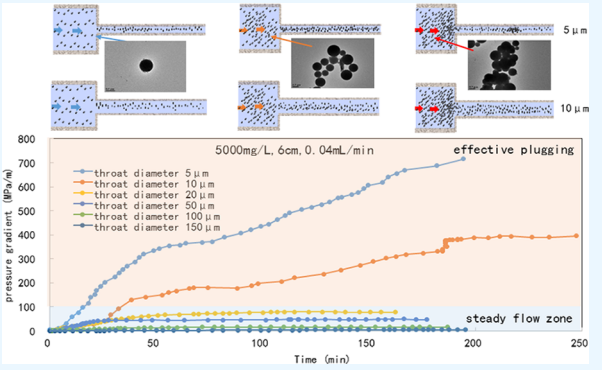

1. INTRODUCTION

The matrix of low-permeability oil reservoirs is very dense, and generally, fractures are commonly developed, leading to strong heterogeneity of the reservoir, which is easy for water channeling to occur during the development process; especially for oil reservoirs with edge water supply, severe water channeling often leads to low oil recovery.[1,2] The plugging technology, as a leading technology for effectively improving oil recovery in heterogeneous reservoirs, has always been a hot research topic in the petroleum industry. Among them, granular plugging agents with special functions and their plugging technology have developed rapidly.[3−9]

According to the characteristics of water channeling treatment in low-permeability heterogeneous oil reservoirs, previous research mainly focused on the direct plugging or bridge plugging of polymer microspheres in the large pores under laboratory conditions during the migration of polymer microspheres to the deep part of the reservoir and achieve the purpose of plugging the water breakthrough channel. However, this kind of plugging is often concentrated near the injection end, it is difficult to move to the deep part of the reservoir smoothly, and it is difficult to effectively plug the water channeling channel far away from the injection well.

Ma et al. studied the polyacrylamide microspheres that can absorb and expand; they used the swelling characteristics of

Received: April 23, 2023
Accepted: May 23, 2023
Published: May 31, 2023

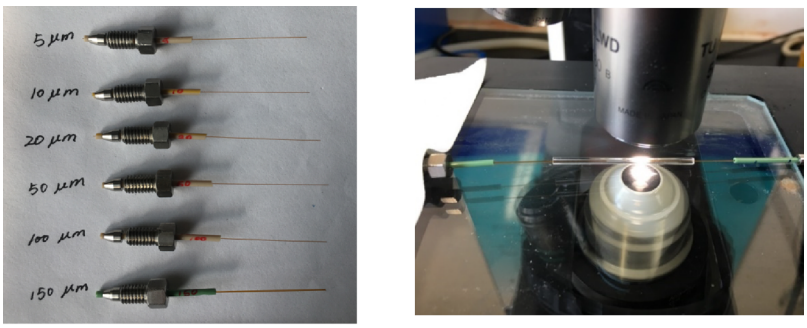

a) microcapillary pore models b) outlet flow rate observation

Figure 1. Microcapillary models for the plugging experiment.

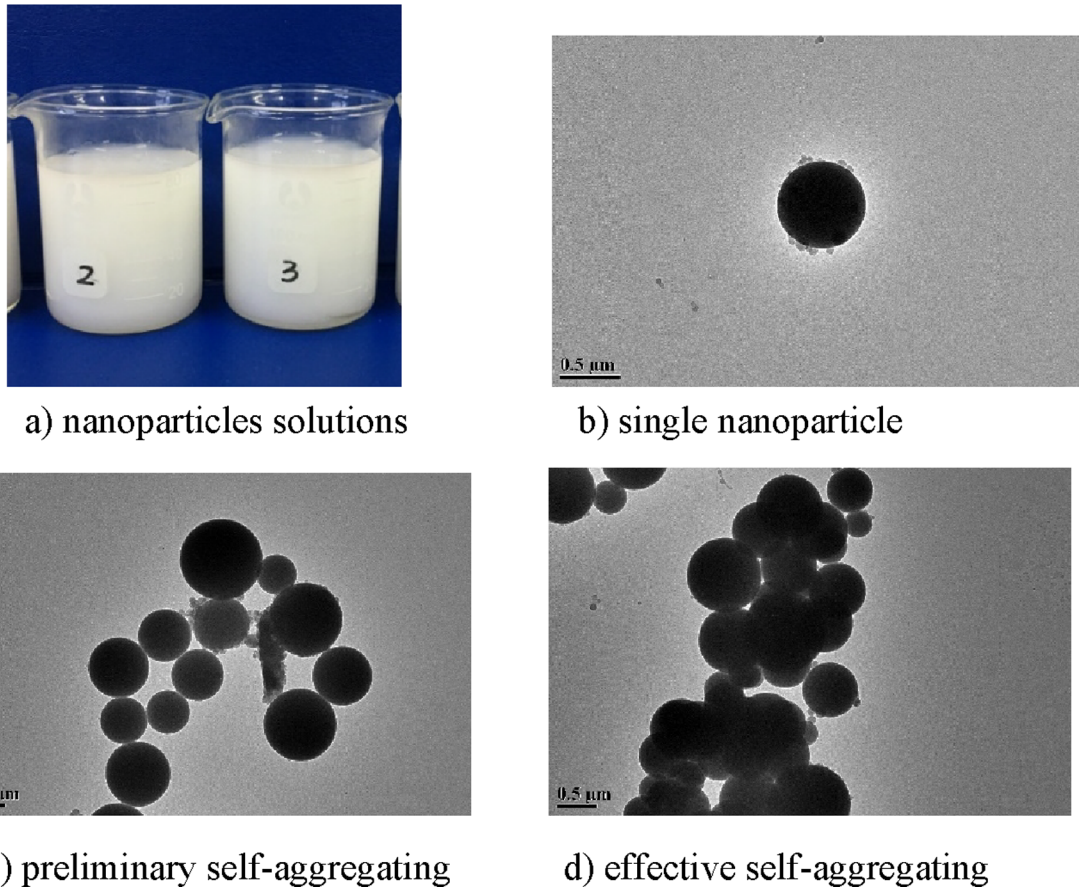

Figure 2. TEM images of controllable self-aggregating nanoparticles.

microsolvity to plug the water breakthrough channels of heterogeneous reservoirs and injected the microspheres into the heterogeneous reservoir before swelling, and then the polyacrylamide microspheres continued to expand under the action of formation water to form larger particle size microspheres and then plug the high-permeability layer.[10−12] However, this swellable polyacrylamide microsphere has the problem of shearing and being easily broken, resulting in a poor actual profile control effect. Yang et al. found that microspheres synthesized by acrylamide as monomers have poor temperature resistance and are prone to thermal decomposition at high formation temperatures, which limits its application in high-temperature heterogeneous reservoirs.[13−15]

In order to achieve deep profile control in low-permeability heterogeneous reservoirs, it is necessary to solve the sharp contradiction between the migration and plugging of profile control agents in the reservoir. As a reservoir with porous media, its most basic channels are pores and throats (including fractures); that is, the most basic unit of profile control agent migration and plugging is the pore throat. This studies the migration and plugging mechanism of a new type of profile control agent, controlled self-aggregating nanoparticle (CSA), in the pore throat microcapillary model, attempting to reveal the essential reason why CSA truly achieves deep profile control in reservoirs.

The injection of controllable self-aggregating nanoparticles into heterogeneous reservoirs will be influenced by multiple factors. Previous studies only focused on whether the plugging

https://doi.org/10.1021/acsomega.3c02775
ACS Omega 2023, 8, 21305−21314

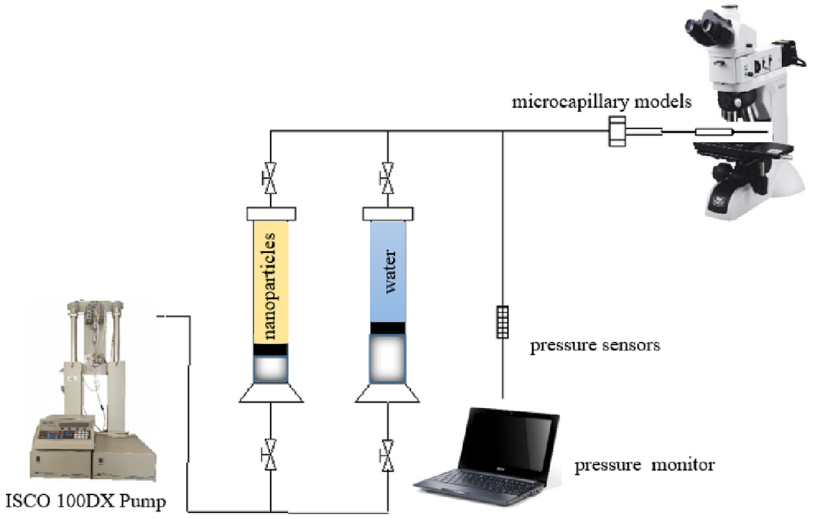

Figure 3. Flowchart of the nanoparticle plugging experiment.

Table 1. Experimental Parameter Design

no.	injection rate (mL/min)	particle size (nm)	concentration (mg/L)	microtubule length (cm)	pore throat diameter (μm)
1	0.02	500	2000	6	5/10/20/50/100/150
2	0.03	500	2000	6	5/10/20/50/100/150
3	0.04	500	2000	6	5/10/20/50/100/150
4	0.02	500	2000	12	5/10/20/50/100/150
5	0.03	500	2000	12	5/10/20/50/100/150
6	0.04	500	2000	12	5/10/20/50/100/150
7	0.02	500	5000	6	5/10/20/50/100/150
8	0.03	500	5000	6	5/10/20/50/100/150
9	0.04	500	5000	6	5/10/20/50/100/150
10	0.02	500	5000	12	5/10/20/50/100/150
11	0.03	500	5000	12	5/10/20/50/100/150
12	0.04	500	5000	12	5/10/20/50/100/150

agent and profile control agent could achieve a certain plugging strength, and the evaluation indicators in the laboratory were generally based on specific evaluation conditions and specific profile control agents. However, the effects of the actual performance parameters and injection conditions of CSA on the plugging channel and plugging strength have not been thoroughly studied in the actual application process. The evaluation of the effect of controlling water breakthrough channels is generally limited to the increase in the ultimate recovery rate of the reservoir but often ignores the influence of changes in reservoir pores during the different injection and production stages and different profile control displacement cycles in heterogeneous reservoirs on subsequent water flooding. There is no targeted adjustment of the scheme for the heterogeneous reservoir conditions after certain stages of treatment.

Therefore, this paper comprehensively considers the four main factors that affect the deep profile control effect of injectable controllable self-aggregating nanoparticles: particle concentration, injection rate, pore length, and reservoir pore diameter. The resistance coefficient and plugging rate of controllable self-aggregating nanoparticles under different injection parameters were obtained through a cross-experiment. This provides a theoretical guidance and research ideas for solving the problem of profile control agents, such as agents that can inject into the oil reservoir being often unable to plug the water channel or agents that can plug the water breakthrough channels being unable to inject into the oil reservoir.

2. EXPERIMENTAL SECTION

2.1. Materials. The experiment designed different microcapillary models that were sealed and connected by a compression fitting, as shown in Figure 1. It was verified that the model can withstand high pressure and has a sealing characteristic. Microcapillary glass tubes with pore diameters of 5, 10, 20, 50, 100, and 150 μm were inserted into the PEEK tube and fixed by compression fitting.

2.2. Apparatus. This study applied 500 nm-diameter controllable self-aggregating nanoparticles, 2000 and 5000 mg/L nanoparticle solutions, and TEM images of controllable self-aggregating nanoparticles, as shown in Figure 2. PEEK tubes with different inner diameters, pressure sensors, intermediate containers, an ISCO 100DX pump, microcapillaries from Polymicro Technologies (with pore diameters of 5, 10, 20, 50, 100, and 150 μm), and a Nikon Eclipse LV100ND microscope were used. The simulation experiment was conducted under normal-temperature conditions; the experimental flowchart is shown in Figure 3.

2.3. Experimental Procedures. The experimental procedure for the plugging characteristics of nanoparticles in microcapillary pore models is as follows:

(1) Prepare microcapillary pore models with different pore sizes (5, 10, 20, 50, 100, 150 μm) and two different lengths (6

https://doi.org/10.1021/acsomega.3c02775
ACS Omega 2023, 8, 21305−21314

and 12 cm), and assemble the device according to the flowchart in Figure 3.

(2) Use ionized water as the base fluid medium and measure the stable flow pressure at different injection rates of 0.02, 0.03, and 0.04 mL/min.

(3) Prepare a nanoparticle solution with concentrations of 2000 and 5000 mg/L and a nanoparticle size of 500 nm, place the solution in the middle container, and inject it into the microcapillary pore models with different pore sizes at different injection rates (0.02, 0.03, and 0.04 mL/min). Record the pressure and outlet liquid volume changes at different injection times. Use a small amount of silicone oil in the outlet end of the visual tube for sealing and marking to record and observe the outlet volume and prevent liquid evaporation.

(4) Change the nanoparticle concentration, pore length, throat diameter, and injection rate, and then record the pressure and outlet flow rate changes under each experimental condition. Repeat the experimental steps in (1)−(3).

This paper considers the four main factors that affect the plugging effect of injectable controllable self-aggregating nanoparticles: concentration, injection rate, pore length, and pore throat diameter. The resistance coefficient and plugging rate of controllable self-aggregating nanoparticles under different injection parameters were obtained through a cross-experiment. The experimental parameters are as shown in Table 1.

2.4. Predictive Models. The theoretical basis for the prediction model of the injection resistance coefficient and the plugging rate of controllable self-aggregating nanoparticles is based on the application of two methods, gray relational analysis (GRA) and gene expression programming algorithm (GEP).

GRA can statistically analyze the effects of multiple factors and characterize the strength, size, and order of the relationship between factors using the degree of association as a reference based on various sample data of factors.[16] If the degree of association is greater than 0.8, it indicates a good correlation between factors; if the degree of association is between 0.5 and 0.8, it indicates a relatively good correlation between the factors; and if the degree of association is less than 0.5, it indicates that the factors are basically unrelated.[17] By applying the GRA method, the degree of correlation between each influencing factor and the injection resistance coefficient and plugging rate of CSAs is first identified, and a model is established using the stepwise discrimination method, ultimately resulting in a highly accurate prediction model.

The GEP is a recently developed evolutionary method, which is based on the development of genetic algorithms and genetic programming. It overcomes the complexity of function in genetic algorithm systems and the difficulty of genetic operations in genetic programming systems. The GEP has stronger function discovery ability and higher search efficiency and can achieve data mining in multi-dimensional space. It is currently the most effective analytical method for complex multi-factorial relationship problems.[18] Currently, the gene expression algorithm has been used in the prediction of dynamic modulus of asphalt mixtures,[19] the prediction of bond strength of concrete,[20] cost estimation of subway construction projects,[21] and depth prediction of abrasive jet cutting,[22] among other related research, and ideal predictive models have been established to improve prediction accuracy.

This paper for the first time applies this algorithm to the field of oilfield development technology to analyze predictive models under multiple influencing factors. Based on the demand for accurate prediction of the effect of research and application of profile control agents, CSAs with a diameter of 500 nm are studied for their transport behavior in micro-capillary pores. Reliable experimental data is used as the basis for calculations, with nanoparticle concentration (C), injection rate (V), pore length (L), and throat diameter (D) as the main parameters. A prediction model for the injection resistance coefficient (F) and plugging rate (I) of nanoparticles based on the GEP is established to achieve an accurate evaluation and rapid prediction of the application effect of nanoparticles in reservoirs.

3. RESULTS AND DISCUSSION

3.1. Displacement Dynamic Analysis. One set of experimental results was selected for analyzing the displacement flow dynamics of controllable self-aggregating nanoparticles in microcapillary pore models. The pump injection flow rate was 0.04 mL/min. A solution of nanoparticle size 500 nm and concentration 5000 mg/L was injected into a 6 cm-long microcapillary pore model with pore sizes of 5, 10, 20, 50, 100, and 150 μm. The changes in injection pressure and outlet liquid volume were recorded.

As shown in Figures 4 and 5, when the 5000 mg/L nanoparticle solution was injected at a rate of 0.04 mL/min

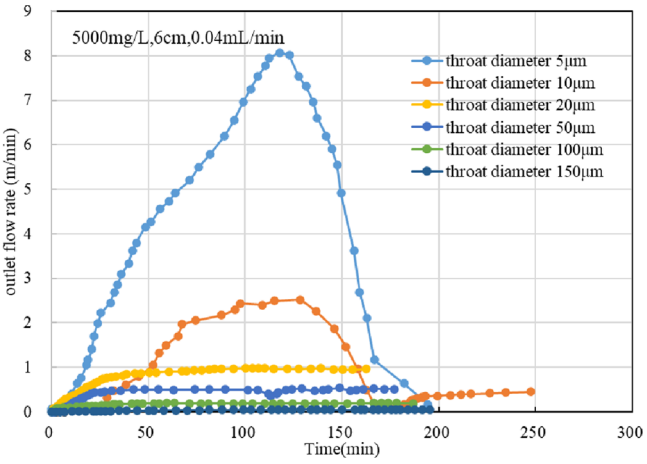

Figure 4. Dynamic diagram of the outlet flow rate.

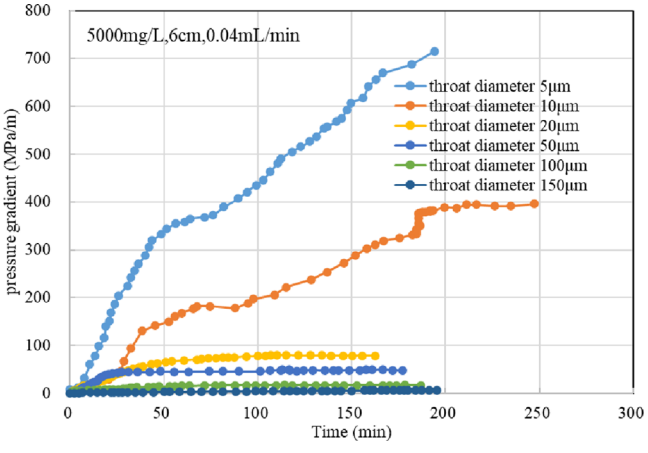

Figure 5. Dynamic diagram of the displacement pressure gradient.

https://doi.org/10.1021/acsomega.3c02775
ACS Omega 2023, 8, 21305−21314

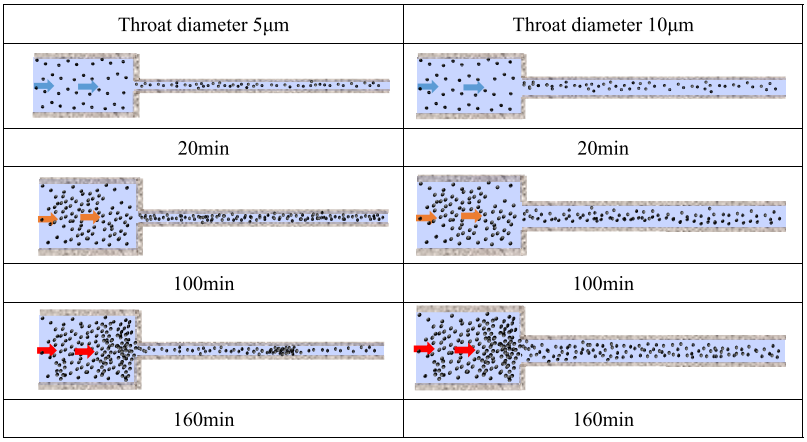

Figure 6. Schematic diagram of flow and plugging in the throat.

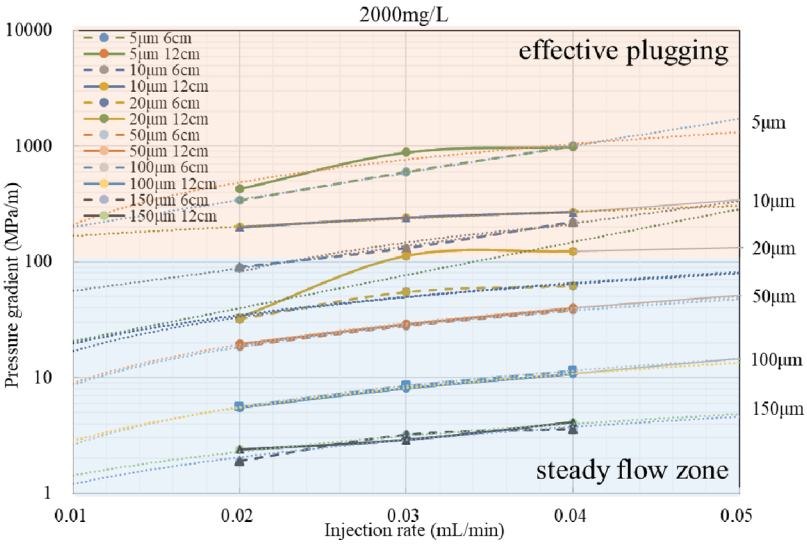

Figure 7. Pressure gradient change at different injection rates (2000 mg/L).

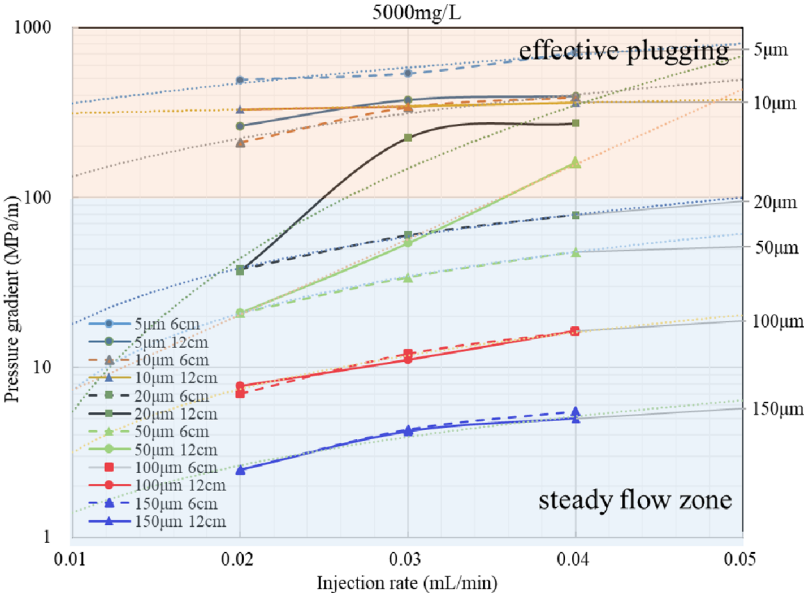

Figure 8. Pressure gradient change at different injection rates (5000 mg/L).

https://doi.org/10.1021/acsomega.3c02775
ACS Omega 2023, 8, 21305−21314

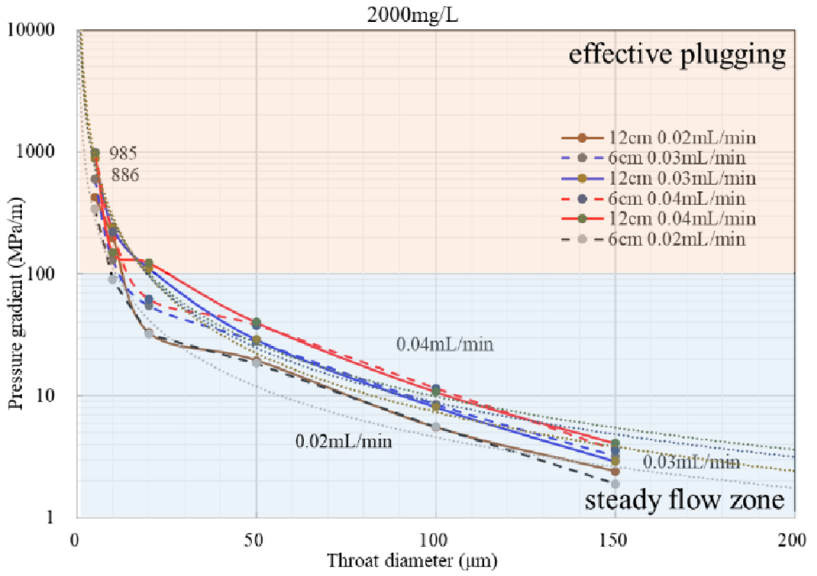

Figure 9. Pressure gradient change at different throat diameters (2000 mg/L).

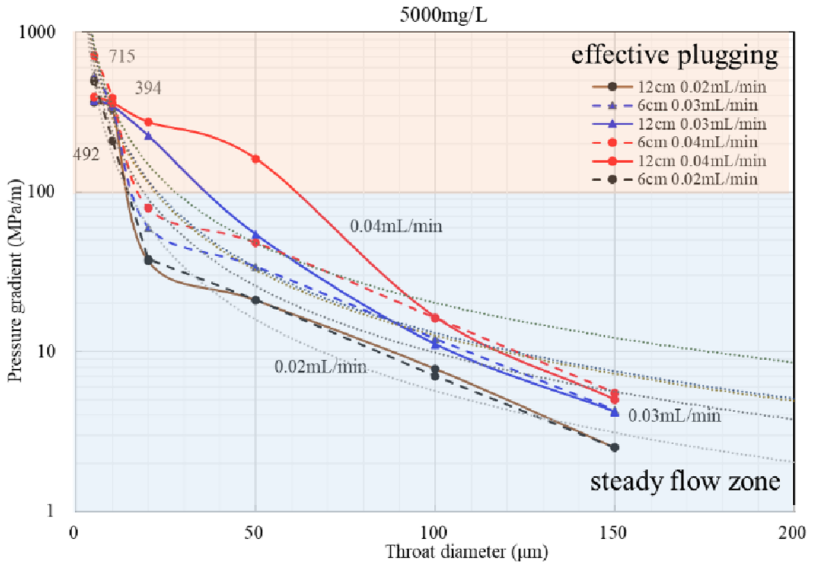

Figure 10. Pressure gradient change at different throat diameters (5000 mg/L).

into the microcapillary pore models with pore diameters of 5 and 10 μm, the outlet flow rate increased continuously within 0−120 and 0−135 min. The pressure gradient also increased rapidly. When the injection pressure gradient reaches 100 MPa/m, the flow rate at the outlet end begins to decrease slowly and the outlet flow decreases with the increase of the injection pressure, which proves that the controllable self-aggregating nanoparticles have achieved effective plugging in the microcapillary. At this time, the nanoparticle solution overcame the capillary resistance and the interfacial tension between solid and liquid to flow forward in the microcapillary pore models.

The outlet flow rate of the microcapillary pore models with a pore size of 5 μm gradually decreased to a very small value within 120−200 min, and the injection pressure gradient stabilized at 715 MPa/m. The microcapillary pore models with a pore diameter of 10 μm entered the stable flow stage of nanoparticles with a gradual decrease in the outlet flow rate within 135−250 min, and the stable flow pressure gradient was 390 MPa/m. As time passed, the outlet flow rate decreased rapidly and the injection pressure gradient tended to stabilize in the microcapillary pore models with pore sizes of 20, 50, 100, and 150 μm. Moreover, as the pore diameter increased, the stable flow pressure gradient decreased. The schematic diagram of flow and plugging in the throat is shown in Figure 6.

3.2. Plugging Effect Analysis. Based on the migration and plugging of nanoparticles in the microcapillary pore models under different experimental conditions, the effective plugging conditions, maximum plugging pressure, and stable flow pressure of nanoparticles under plugging conditions are compared, and the plugging characteristics of nanoparticles in the microcapillary pore models are further analyzed. As shown in Figures 7 and 8, the dashed line represents the 6 cm-length microcapillary experiment and the solid line represents the 12 cm-length microcapillary experiment.

https://doi.org/10.1021/acsomega.3c02775
ACS Omega 2023, 8, 21305−21314

1. The migration and plugging characteristics of nanoparticles in the microcapillary pore model under different concentrations and injection rates can be observed:

(1) As the injection rate increases, the injection pressure gradient increases. When the pore diameter is small, a relatively large injection rate easily causes nanoparticles to plug in the microcapillary pore, and the injection pressure gradient rapidly rises, reducing the injectability of the nanoparticle solution.

(2) When the microcapillary pore diameter is less than 20 μm, the length of the microcapillary (6 cm, 12 cm) has little effect on the injection pressure gradient. When the microcapillary pore diameter is less than 20 μm, the smaller the pore diameter, the greater the influence of the microcapillary length on the injection pressure gradient. This indicates that as the transport length of nanoparticles in small pores increases, the injection pressure gradient increases. The nanoparticles will first enter the larger pores and throats during the injection of the porous medium, thereby achieving to plug the high-permeability water breakthrough channels. As the concentration of nanoparticle solution increases, the injection pressure gradient also increases.

(3) Comparing the flow characteristics and plugging pressure gradient of nanoparticle solutions in the pore model, when the injection pressure is greater than 100 MPa/m under different injection parameters (injection rate, pore length, concentration, pore diameter), the particle solution will form an effective plugging in the microcapillary pore. Therefore, detailed research on the distribution and size of pore throats in oil reservoirs should be done in oilfield acidification and water plugging operations, and based on the experimental results of the laboratory nanoparticle solution transport characteristics, the nanoparticle solution and corresponding injection parameters suitable for the target reservoir conditions can be selected, thereby achieving effective plugging of heterogeneous oil reservoir water channels and deep acidification of oil reservoirs.

2. The plugging characteristics of different pore diameters at different flow rates through microcapillary pore models, as shown in Figures 9 and 10:

(1) For different nanoparticle concentrations, the increase in injection rate affects the injection pressure gradient differently. When the concentration of nanoparticle solution is 5000 mg/L, the effect of increasing injection rate on the pressure gradient is small for the same pore diameter. The smaller the pore diameter, the smaller the influence coefficient of the concentration. When nanoparticles with a concentration of 5000 mg/L are injected into microcapillary pore models at different flow rates, the injection pressure gradient increases significantly with the increase of injection rate. The smaller the diameter, the more obvious the change of pressure gradient with flow rate.

(2) When the pore diameter is less than 20 μm, the change in pressure gradient with diameter within the effective plugging zone changes exponentially. In the steady flow zone, the change of pressure gradient with pore diameter is linear. The larger the diameter, the less pressure gradient is affected by the length of the microcapillary.

(3) Based on the flow characteristics of nanoparticle solutions in the microcapillary pore model, as well as the final plugging pressure gradient and outlet flow rate, it can be seen that under different injection parameters (injection rate, microcapillary length, concentration), when the microcapillary diameter is less than 20 μm, the pressure gradient of the injected nanoparticle solution under different parameters increases exponentially as the microcapillary diameter decreases. This indicates that a 500 nm nanoparticle solution can be applied to a heterogeneous oil reservoir channel with pore throats larger than 20 μm by adjusting the injection parameters. During the injection process of nanoparticle solution, it is important to prevent the solution from entering smaller pore throats, which enables the nanoparticle solution to exhibit selective plugging characteristics during the injection process in heterogeneous oil reservoirs. This can improve the displacement profile of the heterogeneous oil reservoir in the subsequent water flooding process and increase the utilization of reserves in low-permeability areas of heterogeneous oil reservoirs.

3.3. Gray Correlation Analysis. The statistical characteristics of the cross-experimental data results were obtained through calculations, as shown in Table 2.

Table 2. Statistical Characteristics of Experiment Data

parameter	C	D	L	V	F	I
minimum value	2000	5	6	0.02	1.93	0.48
maximum value	5000	150	12	0.04	1000	1
average value	3500	55.83	9	0.03	163.47	0.92
median value	3500	35	9	0.03	46.67	0.98
standard deviation	1510.53	53.32	3.02	8.22	243.34	0.13

To determine the degree of influence of the nanoparticle concentration (C), injection rate (V), injection pore length (L), and pore diameter (D) on the injection resistance coefficient (F) and plugging rate (I) of nanoparticles, gray correlation analysis is used for data analysis and the steps of relevant calculations are as follows:

(1) Determine the analysis sequence. In this paper, the resistance coefficient (F) and plugging rate (I) are taken as the mother sequence $Y = Y(k)$, and the four parameters C, V, L, and D are taken as sub-sequences, i.e., i = 1,2,3,4,5,6; k = 1,2,...,72.

(2) Normalize the data sequence into a dimensionless and normalized form. Commonly used methods for calculation include the mean method and initial value method. In this paper, the initial value method is used. $xi(k) = Xi(k)/Xi(1)$.

(3) Obtain the difference sequence, maximum difference, and minimum difference of the relevant data. That is,

$$X_0(k) - X_i(k) \quad (k = 1 \ldots m,\ i = 1 \ldots n,$$

n is the number of evaluation objects)

$$\min_{i=1}^{n}\min_{k=1}^{m}|X_0(k) - X_i(k)| + \max_{i=1}^{n}\max_{k=1}^{m}|X_0(k) - X_i(k)|$$

(4) Calculate the correlation coefficient; the calculation formula is

https://doi.org/10.1021/acsomega.3c02775
ACS Omega 2023, 8, 21305−21314

$$\zeta_i(k) = \frac{\min_i \min_k |X_0(k) - X_i(k)| + \rho \min_i \min_k |X_0(k) - X_i(k)|}{|X_0(k) - X_i(k)| + \rho \max_i \max_k |X_0(k) - X_i(k)|} \quad (12-5) \quad k = 1 \ldots m$$

where resolution coefficient $\rho = 0.5$.

(5) Calculate the degree of relevance; the calculation formula is

$$r_i = \frac{1}{n} \sum_{k=1}^{n} \zeta_i(k)$$

(6) Sort the correlation of each influencing factor. Sort the correlation between the comparison sequence and the reference sequence in descending order.

By analyzing the experiment data, the correlation ranking of the influencing factors on the injection resistance coefficient and plugging rate was obtained, as shown in Table 3. The

Table 3. Correlation of Each Influencing Factor

Parameter	V	L	C	D
resistance coefficient correlation	0.9227	0.9219	0.9096	0.6732
Parameter	L	V	C	D
plugging rate correlation	0.9632	0.9628	0.9488	0.6929

correlation ranking of the four parameter pairs with the resistance coefficient from strongest to weakest is $V > L > C > D$, which means the main factors affecting the injection performance of the nanoparticles are injection rate > pore length > concentration > pore diameter. The correlation ranking of the plugging rate from strongest to weakest is $L > V > C > D$, which means the main factors affecting the plugging rate of the nanoparticles are pore length > injection rate > concentration > pore diameter.

3.4. GEP Analysis. To establish the model using GEP, GeneXproTools was used to select various parameters such as the number of genes, chromosomes, and connection functions. After choosing an evolutionary generation of 3000, a relatively accurate prediction model for injection resistance coefficient and plugging rate was obtained. Multiple function sets were used, and the variable set was $T = \{d0, d1, d2, d3\}$, where d0–d3 represent C, D, L, and V, respectively, to calculate different output values of resistance coefficient (F) and plugging rate (I).

According to the genetic algorithm, the accuracy of the prediction model for the injection resistance coefficient and plugging rate considering four influencing factors is shown in Table 4 in terms of mean square error and correlation

Table 4. Correlation Degree of Each Influencing Factor

modeling results	R^2	correl. coeff
resistance coefficient	0.92	0.96
plugging rate	0.87	0.93

coefficient of calibration. The data shows that the obtained prediction model can well predict the values of the injection resistance coefficient and plugging rate under different parameters.

3.5. Predictive Model Results Analysis. For the feasibility and accuracy analysis of using GEP to predict the injection resistance coefficient and plugging rate of controllable self-aggregating nanoparticles, five evaluation indices, determination coefficient (R^2), mean squared error (MSE), residual standard error (RSE), root mean square error (RMSE), and mean absolute error (MAE), were selected to assess the accuracy and reliability of the model calculation results. The calculation formulas for each evaluation index are as follows:

1 Determination coefficient: $R^2 = 1 - \frac{\sum_i (\hat{y}_i - y_i)^2}{\sum_i (\overline{y}_i - y_i)^2}$

2 Mean squared error: $\mathrm{MSE} = \frac{1}{m} \sum_{i=1}^{m} (y_i - \hat{y}_i)^2$

3 Residual standard error:

$$\mathrm{RSE} = \sqrt{\frac{1}{n-p-1}\mathrm{RSS}} = \sqrt{\frac{1}{n-p-1} \sum (y_i - \hat{y}_i)^2}$$

4 Root mean square error: $\mathrm{RMSE} = \sqrt{\frac{1}{m} \sum_{i=1}^{m} (y_i - \hat{y}_i)^2}$

5 Mean absolute error: $\mathrm{MAE} = \frac{1}{m} \sum_{i=1}^{m} |(y_i - \hat{y}_i)|$

In the formula, $y_i - \hat{y}_i$ represents the difference between the true value and the predicted value on the test set, $n - p - 1$ represents the degree of freedom, and p represents the number of features. Based on the formula, the evaluation indicators for the injectivity resistance coefficient and plugging rate of controllable self-aggregating nanoparticles can be obtained, as shown in Table 5.

Table 5. Evaluation Index of the Prediction Model

evaluation index	R^2	MSE	RSE	RMSE	MAE
injectivity resistance coefficient	0.92	0.74	0.76	0.911	0.98
plugging rate	0.87	0.70	0.88	0.85	0.93

To select the optimal predictive model, the above five indicators are normalized to obtain an expression for the comprehensive evaluation accuracy: $K_i = \frac{1}{n} \sum_{j=1}^{n} \min(E_j)/E_{ij}$, where K_i represents the evaluation accuracy of the ith combination, $i = 1,2, \ldots m$, E_i represents the jth error indicator value of the ith combination, $j = 1,2,\ldots n$, and $\min(E_j)$ represents the minimum value of the jth error indicator value among the m combinations. The larger the prediction accuracy K_i, the better the corresponding combination prediction model. According to the results of the comprehensive evaluation accuracy calculation, the prediction model calculated by the GEP has an accuracy of 0.91 for the injection resistance coefficient and an accuracy of 0.93 for the plugging rate of controllable self-aggregating nanoparticles. The predicted values of the injection and plugging properties under different experimental parameters are calculated by the program, as shown in Figure 11.

4. CONCLUSIONS

By studying the plugging characteristics of controllable self-aggregating nanoparticles, a microcapillary pore model was established to investigate the plugging characteristics exhibited by different injection parameters. The critical conditions for effective plugging of controllable self-aggregating nanoparticles in pores were determined, and predictions were made regarding the resistance coefficient and plugging rate of

https://doi.org/10.1021/acsomega.3c02775
ACS Omega 2023, 8, 21305−21314

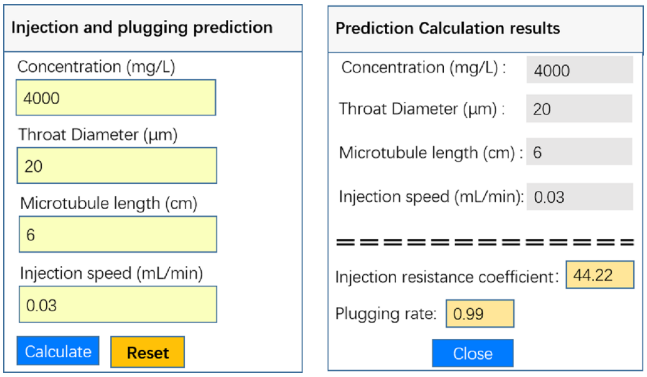

Figure 11. Calculation results of the injectability prediction model.

nanoparticles in pores. The following insights and conclusions were obtained:

1. Based on microcapillary pore model experiments, it was found that when the injection pressure in the pore model was greater than 100 MPa/m under different injection parameters (injection rate, pore length, concentration, and pore diameter), an effective plugging of particle solution would form in the pore. When the microcapillary diameter was small, a relatively large injection flow rate could easily cause particle plugging in the microcapillary pores, resulting in a rapid increase in the injection pressure gradient, which in turn reduces the injectivity of the particle solution. As the particle transport length increased in small pores, the injection pressure gradient increased, and the nanoparticles would preferentially enter larger pores and throats during the injection process in porous media, thereby achieving plugging of high-permeability flow channels. As the particle concentration in the solution increased, the injection pressure gradient also increased.
2. The 500 nm nanoparticle solution used in the experiment could be applied to pore throats larger than 20 μm in heterogeneous reservoir water flow channels by adjusting the injection parameters. During the nanoparticle injection process, the nanoparticle solution could not enter smaller pore throat spaces, resulting in selective plugging characteristics of nanoparticles during injection in heterogeneous reservoir pores.
3. Using cross-experimental data, the main parameters affecting the nanoparticle injection resistance coefficient and plugging rate were selected, including nanoparticle concentration, injection rate, pore length, and pore diameter. A fast and accurate prediction model for particle injection resistance coefficient and plugging rate was established. The gray correlation analysis method was introduced to determine the main factors affecting the injectivity of nanoparticles, in order of strength from high to low: injection rate > pore length > concentration > pore diameter. The main factors affecting the plugging rate of nanoparticles were in order of strength from high to low: pore length > injection rate > concentration > pore diameter.
4. The GEP was introduced, and after 3000 iterations, a reasonable and accurate prediction model was obtained. The relationship between the controllable self-aggregating nanoparticle injection resistance coefficient and plugging rate and the four main controlling factors was determined. The prediction model obtained using the GEP was evaluated using multiple evaluation criteria and comprehensive evaluation considerations. The accuracy of the controllable self-aggregating nanoparticle injection resistance coefficient is 0.91 and that of the plugging rate is 0.93 in the prediction models.

AUTHOR INFORMATION

Corresponding Author

Xiangan Yue − *State Key Laboratory of Petroleum Resources and Prospecting, China University of Petroleum (Beijing), Beijing City 102249, China; College of Petroleum Engineering, China University of Petroleum (Beijing), Beijing 102249, China;* orcid.org/0009-0005-1743-220X; Email: yang1986zhi@126.com

Authors

Zhiguo Yang − *State Key Laboratory of Petroleum Resources and Prospecting, China University of Petroleum (Beijing), Beijing City 102249, China; College of Petroleum Engineering, China University of Petroleum (Beijing), Beijing 102249, China;* orcid.org/0000-0002-1008-1903

Minglu Shao − *School of Petroleum Natural Gas Engineering, School of Energy, Changzhou University, Changzhou City 21306, China*

Shanshan Gao − *Engineering Technology Research Institute of Huabei Oilfield Company, PetroChina Company Limited, Beijing 062552, China*

Complete contact information is available at: https://pubs.acs.org/10.1021/acsomega.3c02775

Notes

The authors declare no competing financial interest.

ACKNOWLEDGMENTS

This work was financially supported by the National Science and Technology Major Projects (2017ZX05009-004), National Science and Technology Major (2016ZX05050012), National Natural Science Foundation of China (51334007), and National Natural Science Foundation of Jiangsu Province (BK20220622).

REFERENCES

(1) Zhang, Y.; Feng, Y.; Li, B.; Han, P. Enhancing oil recovery from low-permeability reservoirs with a self-adaptive polymer: A proof-of-concept study. *Fuel* **2019**, *251*, 136−146.

(2) Hao, H.; Hou, J.; Zhao, F.; Song, Z.; Hou, L.; Wang, Z. Gas channeling control during CO_2 immiscible flooding in 3D radial flow model with complex fractures and heterogeneity. *J. Pet. Sci. Eng.* **2016**, *146*, 890−901.

(3) Yang, Z.; Yue, X.; Shao, M.; Yue, T.; He, J. Performance evaluation and self-aggregation plugging characteristic of nano microspheres as profile control agent. *Xinan Shiyou Daxue Xuebao, Ziran Kexueban* **2021**, *43*, 178−186.

(4) Shao, M.; Yue, X.; Yue, T.; He, J. Preparation and evaluation of anti-temperature and anti-shearing microspheres profile control agent. *Fault-Block Oil & Gas Field* **2020**, *27*, 399−403.

(5) Li, Q.; Yue, X.; Yang, C.; Tian, W.; Kong, B. Effect of effective distance of polymer microspheres on profile control:a case study of Gao qian nan reservoir. *Duankuai Youqitian* **2018**, *25*, 262−265.

(6) Pu, W.; Zhao, S.; Mei, Z.; Yang, Y. Experimental study on profile control and oil displacement of polymer microspheres/polymer under heterogeneous conditions. *Shiyou Kantan Yu Kaifa* **2018**, *8*, 61−65.

(7) Shao, M.; Fu, L.; Yue, X. Experimental study on aggregation regulation and plugging performance of nanoparticles in low-permeability heterogeneous cores. *ChemistrySelect* **2022**, *7*, No. e202104085.
(8) Shao, M.; Gu, F.; Fu, L.; Yue, X. Synthesis and In-Situ Aggregation Plugging Capacity of Nanoparticles as Potential Deep Profile Control Agents. *ChemistrySelect* **2022**, *7*, No. e202201486.
(9) Ngouangna, E. N.; Jaafar, M. Z.; Norddin, M. M.; Agi, A.; Oseh, J. O.; Mamah, S. Surface modification of nanoparticles to improve oil recovery Mechanisms: A critical review of the methods, influencing Parameters,advances and prospects. *J. Mol. Liq.* **2022**, *360*, No. 119502.
(10) Yang, H.; Zhao, Q.; Zhao, W.; Zhao, P. Deep profile control and flooding mechanism of nano-scale polymer microspheres based on capillary model. *Duankuai Youqitian* **2020**, *27*, 355−359.
(11) Ma, G.; Shen, Y.; Gao, R.; Guo, X.; Wu, Z. Application properties of nano−/ micro-size acrylamide copolymer microsphere as profile control agent. *Xiandai Huagong* **2016**, *36*, 94−96.
(12) Yu, Z.; Li, Y.; Sha, O.; Su, Z.; Zhou, W. Synthesis and properties of amphiprotic polyacrylamide microspheres as water shutoff and profile control. *J. Appl. Polym. Sci.* **2016**, *133*, 43366.
(13) Yang, H.; Shao, S.; Zhu, T.; Chen, C.; Liu, S.; Zhou, B.; Hou, X.; Zhang, Y.; Kang, W. Shear resistance performance of low elastic polymer microspheres used for conformance control treatment. *J. Ind. Eng. Chem. (Amsterdam, Neth.)* **2019**, *79*, 295−306.
(14) Yang, Z.; Jia, S.; Zhang, L.; Wu, X.; Dou, H.; Guo, Z.; Zeng, L.; Li, H.; Guo, L.; Jia, Z.; et al. Deep profile adjustment and oil displacement sweep control technique for abnormally high temperature and high salinity reservoirs. *Shiyou Kantan Yu Kaifa* **2016**, *43*, 97−105.
(15) Grzelczak, M.; Vermant, J.; Furst, E. M.; Liz-Marzán, L. M. Directed self-assembly of nanoparticles. *ACS Nano* **2010**, *4*, 3591−3605.
(16) Zhang, Q.; Wang, Y.; Cao, X. Backfill strength prediction based on the grey neural network. *Huagong Kuangwu Yu Jiagong* **2011**, *40*, 26−28.
(17) Li, X.; Qian, W.; Cheng, L.; Chang, L. A coupling model based on grey relational analysis and stepwise discriminant analysis for wood defect area identification by stress wave. *BioResources* **2020**, *15*, 1171−1186.
(18) Ferreira, C. Gene expression programming: A new adaptive algorithm for solving problems. *Complex Syst.* **2001**, *13*, 87−129.
(19) Yan, K.; Liu, P.; Wang, X. Prediction of dynamic modulus of asphalt mixture based on gene expression programming algorithm. *Jianzhu Cailiao Xuebao* **2015**, *18*, 1106−1110.
(20) Zhang, R.; Xue, X. Bond Strength Prediction Model of the Near-surface-mounted Fiber-reinforced Polymer Concrete Based on Gene Expression Programming. *Gongcheng Kexue Yu Jishu* **2021**, *53*, 124.
(21) Wang, J.; Lu, Y. Cost estimation of metro tunnel civil engineering based on genetic expression programming. *Changsha Ligong Daxue Xuebao, Ziran Kexueban* **2019**, *16*, 17−24. CNKI:SUN:HNQG.0.2019-03-003
(22) Wang, R.; Zhong, G.; Zhou, W.; Li, L.; Yang, H.; Wang, F. A model for predicting cutting depth of casing using AWJ technique based on gene expression programming algorithm. *Zhongguo Shiyou Daxue Xuebao, Ziran Kexueban* **2015**, *39*, 60−65.

https://doi.org/10.1021/acsomega.3c02775
ACS Omega 2023, 8, 21305−21314